

## EPITHERMAL Au–Ag MINERALIZATION IN TERRIGENOUS STRATA OF THE BASEMENT OF THE PECHALNINSK VOLCANIC DOME STRUCTURE (NORTH-EAST OF RUSSIA)

© 2025 V. M. Kuznetsov<sup>a</sup>, \*, N. E. Savva<sup>b</sup>, \*\*, A. V. Volkov<sup>c</sup>, \*\*\*,  
K. Yu. Murashov<sup>c</sup>, A. L. Galyamov<sup>c</sup>, and A. V. Grigorieva<sup>c</sup>

<sup>a</sup>*Karpinsky All-Russian Scientific Research Geological Institute,  
Saint Petersburg, Russia*

<sup>b</sup>*Shilo North-East Interdisciplinary Research Institute, FEB RAS,  
Magadan, Russia*

<sup>c</sup>*Institute of Geology of Ore Deposits, Petrography, Mineralogy and Geochemistry of the Russian Academy of Sciences,  
Moscow, Russia*

\*e-mail: v\_kuznetsov12@mail.ru

\*\*e-mail: nsavva7803@mail.ru

\*\*\*e-mail: tma2105@mail.ru

Received August 19, 2024

Revised October 02, 2024

Accepted October 28, 2024

**Abstract.** Epithermal Au–Ag mineralization of the Pechalnoe deposit is of considerable interest, since it was formed in carbonaceous terrigenous strata of the basement of a volcanic dome structure, at a distance of about 200 km from the border of the Okhotsk-Chukchi marginal continental volcanic belt. The geological structure of the Pechalnoye deposit is two-tiered: quartz-adularic and quartz Au–Ag veins are localized in keratinized terrigenous rocks of the lower tier, and quartz rhyolites and komendites of the Pechalninsky strata of the upper tier contain potentially industrial REE mineralization. Productive veins form three zones of sublatitudinal strike, the length of the veins in which is 200–300 m, sometimes 640, 840 m; average thickness 0.1–3 m, rarely up to 6.2 m, average contents: Ag — 266 g/t, Au — 4.4 g/t. The following mineralogical features of ores have been established: low sulfidity (1–2%); native Ag, low-grade Au, polybasite, and highly selenic acanthite act as productive minerals, in addition, arsenic pyrite, arsenopyrite, pyrrhotite, ferruginous sphalerite, chalcopyrite and marcasite are quite widely developed in ores. The geochemical features of the ores are in good agreement with the mineral composition. The ores are enriched with a fairly wide range of trace elements (according to the rating): Ag, Au, As, Sb, Se, W, Tl, Li, Be, Bi, Cs, Mo, the predominance of light lanthanides over heavy ones has been established, very low Eu/Sm ratios (<<1), slightly inclined nearchondrite spectra (without distinct European minima or maxima); the ratio of Ce/Ce\* and Eu/Eu\* values indicate oxidative conditions during ore formation; the REE spectra are dominated by light “hydrophilic” lanthanides of the “cerium” group; the REE varies widely. The obtained mineralogical and geochemical data allow us to attribute the mineralization of the Pechalnoye deposit to the selenium subtype of the low-sulfidized class of epithermal deposits. According to geological and mineralogical-geochemical data, the deposit can be classified as poorly eroded, which makes it possible to predict the identification of new ore bodies that do not come to the surface.

**Keywords:** *OChVB, volcanic dome structure, quartz-adular veins, ore textures, epithermal mineralization, mineralogical and geochemical features, gold, silver, model of formation*

**DOI:** 10.31857/S02030306250103e9

## INTRODUCTION

In the northwestern flank of the Khurchan-Orotukan tectonomagmatic activation (TMA) (Fig. 1), in the late 1970s, Au–Ag epithermal deposits Pechalnoe and Vtvistoe were discovered in the Lower Jurassic black shale strata of the basement of volcano-dome structures (VDS). Additionally, in these same VDS, potentially promising industrial occurrences of rare metals and REE in alkaline

rhyolites were identified [Egorov et al., 2005; Volkov et al., 2023, Grigorieva et al., 2024].

The Pechalnoe deposit is located 40 km north of Orotukan settlement in Magadan region, which is situated at the 392 km mark of the Kolyma highway (Fig. 2, inset), originating in Magadan city. In 1980–1989, prospecting and prospecting-evaluation works were carried out at the Pechalnoe deposit by the Seimchan GRE, as a result of which the forecasted resources of the deposit in category P 1 were estimated at 4 tons of gold and 150 tons of silver (Yachnaya et al., 1990<sup>1</sup>).

The main purpose of this article is to analyze new mineralogical and geochemical data obtained from studying the epithermal Au–Ag mineralization of the Pechalnoe deposit, to determine the relationship between epithermal and REE mineralization; and to refine the ore formation model on this basis.

It should be noted that this work presents for the first time the results of electron microscopy and electron probe microanalysis of ore minerals, as well as geochemical study of epithermal mineralization using X-ray fluorescence (XRF) and ICP-MS analysis methods.

## RESEARCH METHODS

Ore mineralogy was studied in polished sections using an AXIOPHAN Imaging microscope. The chemical composition was determined using electron probe microanalyzers Camebax (analysts E.M. Goryacheva, T.V. Subbotnikova) and QemScan (EVO50) with the Quantax Esprit X-ray energy dispersive microanalysis system at SVKNII FEB RAS, Magadan (analyst O.T. Sotskaya). Identification of ore minerals in comendites was performed on a JSM-5610LV scanning electron microscope (Japan) at the IGEM RAS Shared Research Center (analyst L.A. Ivanova). The electron microscope is equipped with an INCA-Energy 450 energy dispersive analytical spectrometer (Great Britain).

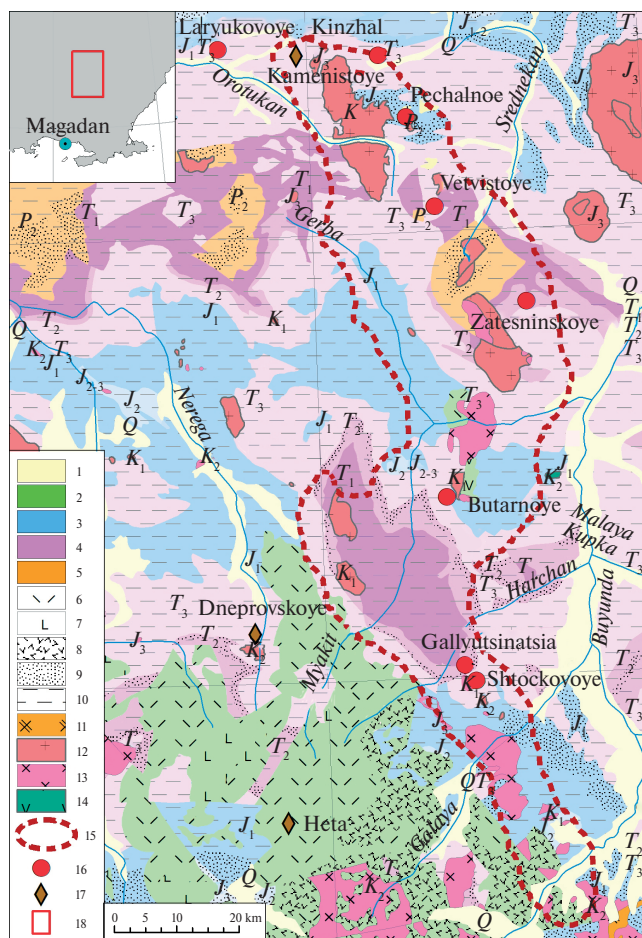


**Fig. 1.** Position of the Pechalninsky VDS in the Khurchan-Orotukan TMA zone. The scheme is compiled on a tectonic basis [Kuznetsov et al., 1993] with additions and simplifications.

1–5 – geological formations: 1 – Quaternary; 2 – Cretaceous; 3 – Jurassic; 4 – Triassic; 5 – Permian; 6–8 – covers and tuffs of Cretaceous volcanics; 9, 10 – sandstones and clayey formations of the Verkhoyansk complex; 11 – syenites; 12 – granitoids; 13 – diorites and granodiorites; 14 – small intrusions of gabbro-diorites; 15 – contours of the TMA areal; 16, 17 – deposits: 16 – gold, 17 – tin ore; 18 – map contour.

<sup>1</sup> Yachnaya V.D., Paraka V.N. et al. Report on the results of prospecting and evaluation work at the Pechalnoe deposit in the Zolotistaya river basin for 1988–1989. Seimchan GRE SVPGO, Seimchan village, Magadan region, 1990. 582 p.

The determination of the concentration of rock-forming and certain trace elements was performed by XRF method on an Axios mAX vacuum spectrometer manufactured by PANalytical at the IGEM RAS Analytical Center for Collective Use (analyst A.I. Yakushev). Trace element measurements (ICP-MS) were carried out on an X-Series II inductively coupled plasma mass spectrometer (analyst Ya.V. Bychkova). Detection limits for elements ranged from 0.1 ng/g for heavy and medium-mass elements, increasing to 1 ng/g for light elements. Gold in samples was determined by atomic absorption spectrometry with electrothermal atomization on a Spectr AA220Z spectrometer (analyst V.A. Sychkova).

To assess the conditions of volcanogenic mineralization formation, geochemical indicators and elemental ratios were determined:  $\Sigma$ REE,  $\Sigma$ LREE,  $\Sigma$ HREE,  $\Sigma$ LREE/ $\Sigma$ HREE, Y/Ho, U/Th, Eu/Eu, Ce/Ce\* and others. Additionally, enrichment coefficients for trace elements in ores were calculated. The obtained values were compiled into tables, which were used to build distribution graphs of REE and other trace elements in the ores of the deposits.

## POSITION OF THE DEPOSIT IN REGIONAL STRUCTURES

In the modern tectonic plan, the Khurchan-Orotukan TMA zone (see Fig. 1) is a zone of deep submeridional fault [Kuznetsov et al., 1993], crossing linear folded structures of the Inyali-Debinsky synclinorium and brachiform structures of the Balygchano-Buyandinsk uplift for more than 200 km. Within its boundaries, ore-bearing VDS are localized (see Fig. 2), fields of dikes and subvolcanic bodies, ore fields with Au–Ag, Au–rare metal, cassiterite-silicate, rare-metal-pegmatite and Ag-polymetallic and REE mineralization.

The Upper Orotukan intrusive-dome structure is confined to the intersection of the Khurchan-Orotukan TMA zone with the transition zone between the Inyali-Debinsky synclinorium and the Balagchano-Buyandinsk uplift (see Fig. 2). In the central part of the structure (see Fig. 1), granitoids of the Upper Orotukan massif of Late Cretaceous age (86 million years, K-Ar

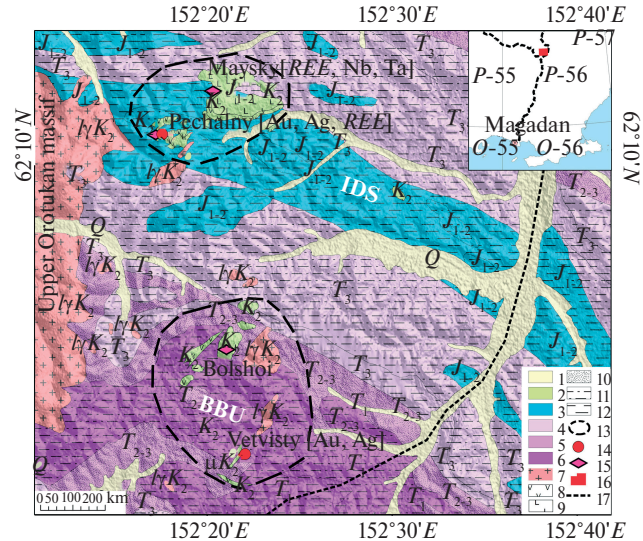


**Fig. 2.** Geological map of the northern part of the Khurchan-Orotukan metallogenetic zone with relief elements according to [Kuznetsov et al., 2008] with modifications.

1 – Quaternary alluvial deposits; 2 – Late Cretaceous alkaline volcanics; 3 – Early-Middle Jurassic black shale strata; 4–6 – terrigenous strata: 4 – Late Triassic, 5 – Middle Triassic, 6 – Early Triassic; 7 – Late Cretaceous granites, granite-porphries; 8 – trachyrhyolites, comendites, 9 – trachybasalts; 10 – sandstones; 11 – siltstones; 12 – argillites; 13 – boundary of volcanic structures; 14, 15 – ore occurrences: 14 – Au–Ag epithermal, 15 – rare metals and REE; 16 – map frame, 17 – federal highway “Kolyma” and its branch “Strelka-Seymchan”. IDS – Inyali-Debinsky synclinorium; BBU – Buyandino-Balygchano anticlinal uplift.

[Kuznetsov et al., 2008]) are exposed on the surface. The massif has a multi-phase structure and represents an oval-shaped body elongated in the submeridional direction (24 × 8 km) in plan view. In the first phase, medium and coarse-grained biotite-hornblende subalkaline granites were formed, and in the second phase – small stocks of granite-porphries, aplites, and fine-grained granites.

The Upper-Orotukan massif gently dips to the east (dip angles 15–45°), and the western contact of the massif is steep (Kuznetsov, 1991<sup>f2</sup>). Several

<sup>2</sup> Kuznetsov V.M. Development of criteria for local forecasting and justification of the optimal direction of geological exploration within the Khurchan-Orotukan zone for gold-silver and silver-polymetallic mineralization // Report on Subject No. 1138 for 1988–1991. Magadan, 1991. 180 p.

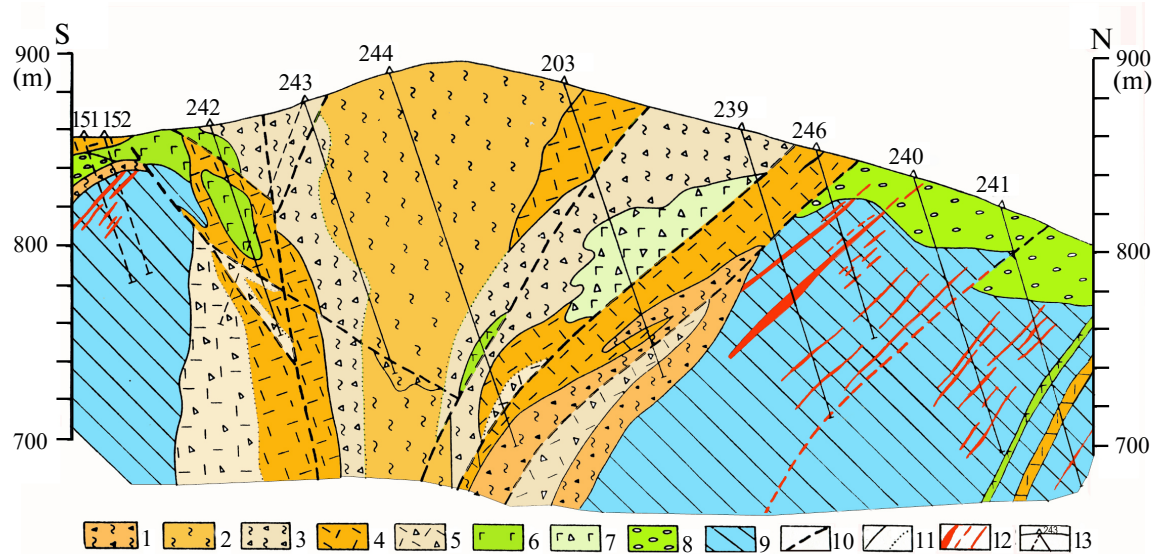


**Fig. 3.** Geological cross-section of Mt. Riolitovaya (Pechalnoe deposit) along the drilling profile, according to (Kuznetsov, 1991<sup>2</sup>) with modifications.

1 – explosive breccias of stage II; 2 – flow-banded rhyolites, comendites and their clastolava; 3 – eruptive breccias of flow-banded rhyolites; 4 – massive rhyolites; 5 – eruptive breccias of rhyolites; 6 – basalts; 7 – tuffs and tuff-conglomerates of basalts; 8 – conglomerates of the lower Pechalninsky strata; 9 – hornfelsed terrigenous rocks; 10 – faults; 11 – boundaries: a – stratigraphic intrusive units, b – facies varieties; 12 – veins and veinlets of quartz-adularia composition; 13 – boreholes and their numbers.

VDSs (volcanic-sedimentary structures) are developed in the supra-intrusive zone of the massif (see Fig. 2). The Pechalnnoye, Vtvistoye ore fields with Au–Ag and Ag-polymetallic mineralization are localized in the terrigenous basement of the latter, while rhyolites and comendites contain potentially commercial concentrations of REE.

The Pechalninsky VDS is located at the intersection of a hidden fault of northwestern strike and the sublatitudinal Laryukovsky fault, along which right-lateral and later left-lateral strike-slip movements of the host rocks occurred.

## GEOLOGICAL STRUCTURE OF THE DEPOSIT

The geological structure of the deposit is two-tiered (Fig. 3): quartz-adularia and quartz Au–Ag veins are localized in hornfelsed terrigenous rocks of the lower tier, while quartz rhyolites and comendites of the Pechalninsky sequence of the upper tier contain potentially commercial rare metal and REE mineralization [Egorov et al., 2005; Volkov et al., 2023; Grigorieva et al., 2024]. The age of quartz-adularia veins, determined

by the K–Ar method, is  $83 \pm 4$  million years (Kuznetsov, 1991<sup>3</sup>).

The block structure of the deposit is formed by variously scaled sublatitudinal, northwestern, and northeastern faults. The oldest, magma-controlling and feeder fault was probably a large fault of northwestern strike that passes through the central part of the deposit. The width of the fault zone is about 0.5 km. This fault, which controls the position of the VDS and dikes, is expressed in a sharp change of positive and negative magnetic fields.

The system of faults (normal faults) of northeastern and northwestern strike, forming a rhomboid block structure of the deposit, is considered as a series of shear fractures in relation to the Laryukovsky fault zone. The width of the fault zone is about 2 km, it includes a system of echelon-arranged faults predominantly dipping south at angles of 65–80°, less often inclined to the north. Meanwhile, productive veins were

<sup>3</sup> Determination of radioisotope age of rocks K–Ar method was performed in the laboratory of isotopic geochronology and geochemistry SVKNII FEB RAS (analysts A.D. Lyuskin, K.K. Novik, N.M. Alexandrova).

formed as a result of strike-slip movements in this zone (Kuznetsov, 1991<sup>2</sup>).

It is assumed that the system of gently inclined (10–30°) to the east and northeast faults, represented by zones of crushing and schistosity with thickness from 0.5 to 10 m, the occurrence of which is determined by the morphology of the submerged roof of the eastern flank of the Upper Orotukan intrusive massif, controls the placement of productive veins (Kuznetsov, 1991f<sup>2</sup>).

### *Host rocks*

In the composition of the Lower Jurassic strata quartz-feldspar siltstones and clay shales predominate. Upper Norian deposits are found locally in the north and south of the ore field and are represented by siltstones with interlayers of clay shales and volcanomictic sandstones with fragments of effusives of medium composition. Terrigenous-sedimentary rocks of the Jurassic and Triassic are dislocated into narrow, sub-latitudinal folds 200–300 m wide, often asymmetrical or isoclinal, sometimes overturned. The dip angles of the fold limbs range from 10° to 80°, mainly 50–70°. Intensive metamorphism of sedimentary rocks is caused by the intrusion of the Upper Orotukan massif and is best traced in clay shales and clay siltstones. At the contact with granite outcrops, biotite-cordierite-quartz and biotite-cordierite-quartz-potassium feldspar hornfels were formed, at some distance from the contact – nodular schists, which are then replaced by spotted schists.

The Pechalninsky strata of volcanics, unconformably overlying the Lower Jurassic deposits, within the VDS forms subhorizontal covers, or fills gentle synclinal basins.

The lower sandy-conglomerate member of the Pechalninsky sequence is overlain by basaltic lava flows of the middle member and the youngest rhyolites of the upper member. The thickness of the lower member is variable and ranges from 1–2 m to 40–55 m. The fine-grained rocks of the member contain imprints of stems and fragments of tree trunks. It is assumed that the deposits of the member represent a facies of volcanic foot hills – lahar, solifluction and lacustrine deposits (Kuznetsov, 1991<sup>2</sup>).

The middle member consists of flows of andesite-basalts and olivine basalts, overlying sandy-conglomerate deposits, sometimes lying directly on dislocated Lower Jurassic rocks. The thickness of the member varies from 10 to 170 m. In terms of chemical composition, the rocks of the member correspond to trachyandesite-basalts [Egorov et al., 2005].

The upper rhyolite member lies with a small break on the basalts, less frequently on the sandstone-conglomerate member. The rhyolite flows in the central part of the VDS are replaced by extrusive facies of complex fluidity. The upper horizons of the flows are composed of massive, sometimes banded rhyolites and their clastolavas.

The rhyolite extrusion of the Pechalninsky VDS (see Fig. 3) was formed in two phases (Kuznetsov, 1991<sup>2</sup>). The marginal parts of the extrusion are composed of rhyolites and clastolavas of the first phase. At the contact with the host sedimentary rocks, bodies of eruptive breccias of the first phase of intrusion are distributed. The central part of the extrusion is composed of fluidal rhyolites, comendites, their clasto lavas and eruptive breccias of the second phase of intrusion (see Fig. 3). The affiliation of these rocks to trachyrhyolites [Egorov et al., 2005] has been established. It was in the latter that potentially industrial concentrations of REE were identified [Volkov et al., 2023].

Metasomatic rocks of the deposit can be attributed to three formations: greisens, secondary quartzites, and propylites.

Greisens are associated with granitoid outcrops, granite-porphyry and rhyolite dikes, as well as hornfelsed sedimentary rocks. In greisens and greisenized rocks, there are veins of gray medium-grained quartz with allotriomorphic-granular texture, containing rare-metal mineralization.

Secondary quartzites within Mount Rhyolite are distributed in the form of an inverted cone, in the central part of which quartz-montmorillonite and quartz-kaolinite facies are developed, within which monoquartzite bodies with a thickness of 5–10 m and a length of up to 50 m are located, confined to fault zones. On the periphery of the cone in the surrounding terrigenous-sedimentary rocks, which are hornfelsed and greisenized, metasomatites of quartz-sericite-hydromica facies

are developed, which are replaced by low-temperature propylites.

Quartz-adularia metasomatites. In some areas, fine-grained aggregates of quartz-adularia metasomatites replace the above-mentioned facies of secondary quartzites. Quartz-adularia metasomatites are associated with productive veins of the same composition.

Propylites are developed in the basalt sequence of the Late Cretaceous-Paleogene, in the deposits of the Lower Jurassic in the eastern part of the area, and are found among metasomatites of other formations. Based on mineral parageneses, medium- and low- temperature propylites are distinguished.

### *Morphology of ore bodies*

The ore-bearing veins of the Pechalnoe deposit were formed in two stages (Kuznetsov, 1991f<sup>2</sup>). The first stage is associated with the formation of intrusions of leucocratic granite formation and comagmatic dikes of the Late Cretaceous; the second – with the formation of the VDS. Veins of stage I – gray medium-grained quartz, are located in greisens and greisenized rocks and are accompanied by tin mineralization. Quartz and quartz-adularia veins of stage II with productive Au–Ag mineralization are of industrial importance. The largest veins are located in the marginal part of the VDS in sedimentary rocks of the Lower Jurassic, within the quartz-sericite-hydromica facies and partly quartz-montmorillonite facies of secondary quartzites. The sublatitudinal strike of the veins and dip to the south at angles of 50–75° predominate. As the distance from the rhyolite extrusion increases in plan and depth, the amount of adularia in the veins decreases, and colloform-banded textures are replaced by spotty and massive ones (Kuznetsov, 1991f<sup>2</sup>).

Productive veins are combined into 3 ore zones: northern, central, and southern, each with a thickness of 350–400 m (Kuznetsov, 1991f<sup>2</sup>), separated by relatively barren intervals with a width of 250–300 m. The northern zone has the shortest extent and is represented by a series of echeloned quartz and adularia-quartz veins. Productive veins of the central zone have predominantly

northeastern strike and can be traced under the deposits of the Pechalninsky formation. Five ore veins (No. 2, 3, 5, 10, 27) and a thick (up to 6.8 m) hydrothermal-metasomatic quartz deposit formed in the delamination plane at the boundary between the Jurassic formation and volcanics have been identified here. The most powerful and productive southern zone combines ore-bearing veins (No. 1, 4, 4 a, 4 b, 5), which contain the main reserves and resources of gold and silver. The length of the veins is usually no more than 200–300 m, in isolated cases 640 m (No. 5) and 840 m (No. 4). The thickness varies from 0.1 to 3 m, occasionally up to 6.2 m (No. 2). The veins represent a series of lenticular echelons with relatively small displacements, sometimes splitting (No. 4) and accompanied by feathering apophyses (No. 4 a, 4 b).

## TEXTURAL FEATURES OF THE ORES

In the productive veins of the Pechalnoe deposit, a combination of framework-lamellar and colloform-banded, as well as breccia and breccia-drusy textures predominate (Fig. 4). In addition, complex, combined textures that represent “composite” formations have been identified in the veins. In different sections of such veins, the ratio of quartz to host rock fragments varies from 1:10 to 10:1 and within even wider limits. In some areas of the veins, breccias are common, in which the fragments are represented by varieties of early-generation quartz (see Fig. 4c), and the cement by late metacolloidal quartz.

Combinational (composite) textures. For the ore-bearing veins of the Pechalnoe deposit, transitions from breccia to lamellar-framework and crustification textures are noted; in places, elements of cockade, drusy, and comb textures are observed (see Fig. 4a).

Frame-lamellar texture is usually developed in the central part of veins (see Fig. 4a), represented by subparallel elongated lamellar aggregates of quartz, rotated relative to each other at an angle of 30° and up to 60°, which form frames in the shape of triangles or quadrangles. Adularia may also participate in the structure of frames. Inside, the

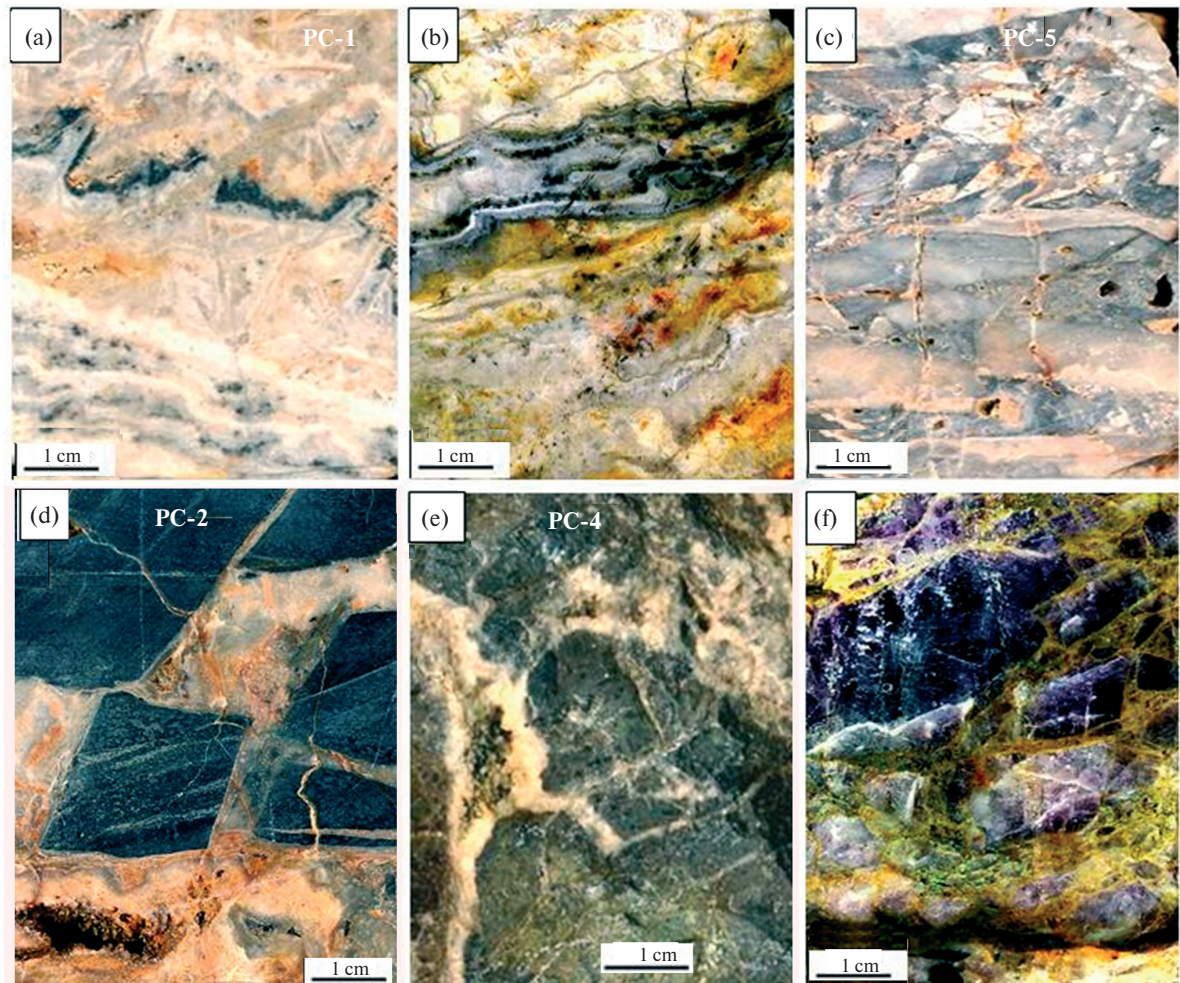


**Fig. 4.** Textures of ores from the Pechalnoe deposit.

a, b – combination of collomorphic-banded and frame-lamellar textures; c – breccia with angular fragments of bleached rhyolite; d – breccia with hornfels fragments in quartz cement and drusy texture in cavities; e – tuffisite according to V.M. Kuznetsov (1991f) with carbonate stringers; f – breccia with large fluorite fragments in tuffisite matrix. PC-1 and others correspond to numbers in tables 3 and 4, as well as sampling locations – PC-1, trench-701(E), zh-1, level 860 m; PC-2, trench-701(E), host rocks, level 860 m; PC-4, K-713, level 750 m; PC-5, K-725(S), level 720 m.

frames are filled with aggregates of collomorphic quartz with traces of gel recrystallization. Polygonal voids are observed between the rotated blocks of plates. Newly formed quartz crystals grow from the walls of the frames inward, forming a drusy texture. In the frame-lamellar texture of the Pechalny deposit, despite the structured space, chalcedony begins to form not only linear but also festooned bands (see Fig. 4a, 4b). The vein aggregate of frame-lamellar texture rarely contains ore mineralization.

Collomorphic-banded texture is associated with the pulsating nature of inflow and boiling of hydrothermal solutions. It serves as an important

prospecting indicator of ore shoots (bonanzas). The black bands composed of ore minerals in such a texture are called “ginguro” (see Fig. 4a, 4b).

Drusy textures form in unfilled cavities, often found in the central part or selvages of veins and between fragments in breccias (see Fig. 4d). In the final stages of ore formation, well-formed crystals of quartz, carbonate, and in productive veins often ore minerals (fahlore, sulfides, native silver and/or native gold) are deposited on the walls of such cavities.

Breccia textures. The vein bodies of the Pechalnoe deposit are characterized by true breccia textures, which feature angular and variable

shapes and sizes of fragments (see Fig. 4c, 4d, 4f), completely enclosed in quartz-adularia, chalcedony, or tuffizite cement. The composition of the fragments often does not correspond to the host rocks on the sides, as the movements of tectonites could be quite significant, resulting in mixing of crushed material from different layers and rocks.

The earliest bodies of pre-ore breccias with angular fragments of hornfelsed sedimentary rocks are located around the field of Late Cretaceous volcanics and are represented by knee-branching vein bodies (see Fig. 4d). Ore breccias include those with fragments of dark purple fluorite in carbonate-chlorite (tuffizite) cement (see Fig. 4f). The textures of late (post-ore) breccias are distinguished by the presence of fragments of volcanic glass, quartz-adularia metasomatites, and productive colloform-banded quartz (see Fig. 4d). They are typically confined to the central part of the deposit and form vein-like bodies up to 2 m thick, sometimes crossing earlier breccias. Post-ore breccias are characterized by the presence of angular fragments (0.5–15 mm) of argillites, basalts, bleached rhyolites, volcanic glass, quartz-adularia metasomatites, and ore-bearing quartz, immersed in a basal (about 30% of the rock volume) tuffizite matrix. According to V.M. Kuznetsov (1991<sup>f2</sup>),

tuffizite is formed by dark gray clay material replaced by secondary chlorite, hydromica, or fine-grained quartz-adularia aggregate, crossed by thin carbonate veinlets (see Fig. 4e).

## MINERALOGICAL CHARACTERISTICS OF ORES

Ore minerals are characterized by small segregations of 0.5–0.05 mm, concentrated in bands of chalcedony colored dark by ore mineralization, the so-called “ginguro”, whose thickness varies from fractions of mm to 0.5–1 cm (see Fig. 4a, 4b). The amount of ore minerals in the veins does not exceed 1–2%. The ores contain more than 20 ore minerals (Table 1). The earliest sulfide mineralization is represented by arsenopyrite, pyrite, marcasite, pyrrhotite, chalcopyrite, sphalerite, and stibnite. The productive association is formed by native silver, polybasite, high-selenium acanthite, and low-grade native gold.

### *Gangue minerals*

Quartz – is the main gangue mineral and is represented by three generations: quartz-I fine and medium-grained, cementing hornfels fragments in early breccias, quartz-II II cryptocrystalline and chalcedony-like to chalcedony, participates

**Table 1.** Mineral composition of the Pechalnoe deposit ores

Mineral groups	Main	Secondary	Rare
Gangue	Quartz Chalcedony Fluorite Albite Adularia?	Carbonate Chlorite Sericite	Rutile
Ore	Pyrite Native silver Ag-tetrahedrite Sphalerite Chalcopyrite Chalcocite Polybasite Acanthite (Se up to 16.8 wt. %)	Native Au Arsenopyrite Mackinstryite Galena Marcasite	Hematite Stephanite? Argyrodite Greenockite?
Supergene	Fe hydroxides Acanthite (supergene)	Chlorargyrite	Anglesite

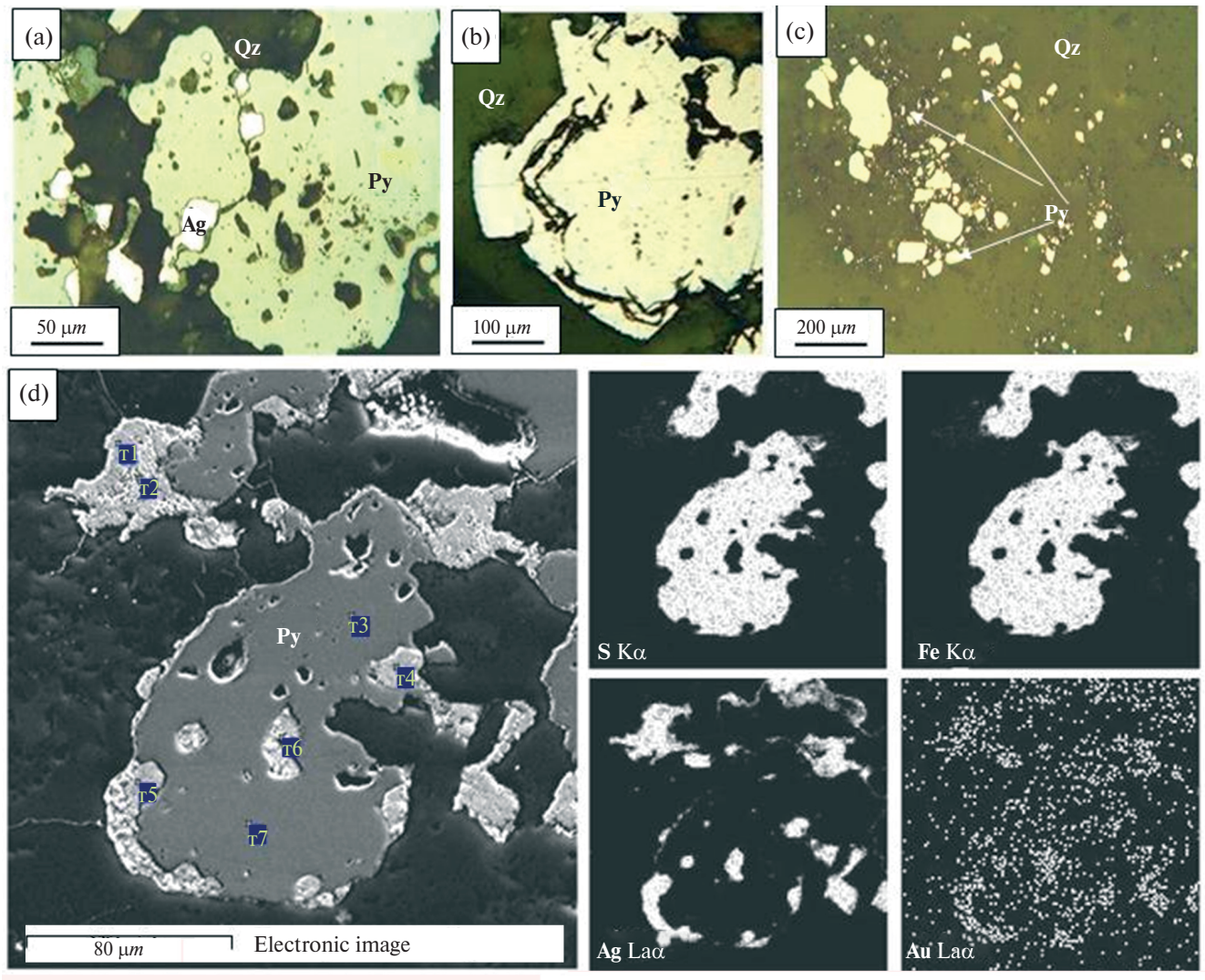


**Fig. 5.** Varieties of pyrite in the ores of the Pechalnoe deposit.  
 a – hypidiomorphic segregation with inclusions of native silver; b – idiomorphic crystals of zonal composition; c – finely disseminated pyrite in metasomatite; d – xenomorphic segregation of pyrite in intergrowth with native silver (electron image and distribution of elements in characteristic radiation).

in the formation of rhythmically banded aggregates to which ore mineralization is confined; quartz-III chalcedony-like forms cement of post-ore breccias.

Albite – is present together with quartz-I in early breccia formations.

Adularia – forms separate rhythms up to 2 mm thick together with quartz-II and chalcedony in *ore* veins of colloform-banded structure.

Fluorite – found as large (up to 3-5 cm) fragments in carbonate-sericite-chlorite cement. Its color is dark purple, characteristic of varieties containing  $\text{TR}^{3+}$ ,  $\text{Eu}^{2+}$  in their composition.

#### Ore minerals

Pyrite – a widely distributed ore mineral, forms hypidiomorphic and idiomorphic inclusions 0.2–0.8 mm in size in ores and metasomatites (Fig. 5c). It often contains droplet-like segregations of golden (Au 3–5 wt. %) native silver (see Fig. 5a, 5d). In some areas (see Fig. 5b), stepped growth of pyrite crystals is observed, indicating an unstable regime of ore formation. Its composition is close to stoichiometric (Table 2).

Sphalerite – forms xenomorphic segregations in quartz, sometimes developing along

**Table 2.** Chemical composition of ore minerals of the Pechalnoe deposit according to microprobe analysis data

Element concentration, wt. %						Formula coefficients					
<i>Pyrite</i>											
S	Fe					S	Fe				
54.25	45.75					2.02	0.979				
52.15	47.85					1.97	1.035				
53.19	46.81					1.99	1.007				
51.54	48.46					1.95	1.052				
<i>Native gold</i>											
Ag	Au										
76.34	23.66										
76.98	23.02										
63.80	36.20										
73.29	26.71										
57.72	42.28										
23.95	76.15										
62.61	37.39										
65.74	34.26										
67.80	32.20										
23.98	76.02										
70.15	29.85										
<i>Rims on low-fineness gold (diffusion of gold into iron hydroxides)</i>											
Ag	Au	Fe	As	O							
26.10	32.47	38.32	3.11								
19.14	24.87	29.57	2.40	24.02							
27.94	41.54	27.43	3.09								
19.07	29.80	19.94	2.21	28.98							
<i>High-selenium acanthite A<sub>2</sub> (S,Se)</i>											
S	Se	Ag	Cu	Ge	Fe	S	Se	Ag	Cu	Ge	Fe
11.64	0	88.36				0.92	0	2.079			
6.38	16.89	76.74				0.53	0.57	1.898			
5.72	15.95	78.33				0.48	0.55	1.969			
14.88	13.84	68.27	3.06		2.01	1.05	0.4	1.438	0.109	0.020	0.382
13.08	1.27	81.83		0.54	1.82	1	0.04	1.861			0.201
6.81	13.29	82.39				0.56	0.44	2.002			
7.27	10.06	81.69				0.61	0.34	2.044			
7.44	13.80	79.20				0.61	0.46	1.930			
12.48	0.58	82.39			1.10	0.99	0.02	1.942			0.113

**Table 2.** *Continued*

Element concentration, wt. %						Formula coefficients					
<i>Argyrodite</i> $Ag_8Ge(S,Se)_6$											
S	Se	Ag	Cu	Ge	Fe	S	Se	Ag	Cu	Ge	Fe
12.35	9.19	76.08	4.10	4.10		4.57	1.38	8.374		0.67	
<i>Mackinstryite</i> $(Ag,Cu,Fe)_2(S,Se)$											
S	Cu	Ag	Se	Fe		S	Cu	Ag	Se	Fe	
12.10	7.97	74.36	5.58			0.90	0.298	1.638	0.17		
13.66	8.95	70.77	6.63			0.98	0.323	1.506	0.19		
13.38	3.25	77.96		3.37		1.00	0.123	1.732	0	0.145	
<i>Chalcopyrite</i> $CuFeS_2$											
S	Fe	Cu				S	Fe	Cu			
35.19	30.55	34.26				2.01	1.002	0.988			
34.54	29.61	34.10				2.01	0.989	1.001			
34.59	28.85	33.73				2.03	0.972	0.999			
34.49	29.48	34.04				2.01	0.987	1.002			
34.63	29.26	34.13				2.02	0.979	1.003			

microfractures (Fig. 6a). Sphalerite intergrows with galena (see Fig. 6c), native silver (see Fig. 6a), with arsenopyrite (see Fig. 6e), as well as with chalcopyrite and acanthite (see Fig. 6f). Individual analyses of sphalerite showed iron content from 5.57 to 6.9 wt. %

Galena – occurs much less frequently than sphalerite, in close association with the latter, forms rims 0.2–0.3 mm on sphalerite (no analytical data available).

Chalcopyrite – is observed everywhere in small (0.5–0.3 mm) xenomorphic segregations and intergrows with polybasite, chalcocite (see Fig. 6b), Ag-tetrahedrite, native silver, and also forms zonal segregations with a chalcocite rim (see Fig. 6b, 6f), thin hypergene rims of acanthite are noted on the outer contour of chalcopyrite segregations. The composition corresponds to stoichiometry (see Table 2).

Polybasite – the most common of Ag minerals, occurs in xenomorphic segregations up to 0.7 mm in size in quartz, intergrows with native silver (see Fig. 6d); a characteristic feature is the emulsion of native silver as a result of photo-etching.

Native silver – a widely distributed mineral in ores, intergrows with sphalerite, pyrite, chalcopyrite, forming rims and inclusions, often with idiomorphic outlines. The composition of native silver contains Au impurities up to 3–5 wt. %.

Native gold – predominantly low-grade (250–300‰), single value – 760‰ (see Table 2). In one of the native gold segregations in oxidized arsenian pyrite, exotic diffusion rims form, consisting of Ag, O, Fe, As (Fig. 7, see Table 2).

Acanthite – a common silver mineral in ores, forms rims on chalcopyrite and sphalerite aggregates (see Fig. 6e), also found as small inclusions in arsenian pyrite (see Fig. 7a), contains high selenium impurity (up to 16‰, see Table 2). High-selenium acanthite is characteristic of epithermal deposits localized in terrigenous black shale strata, such as Rogovik [Savva, 2005; Savva, 2018]. In hypergene acanthite, which forms openwork segregations in oxidized pyrite and thin rims on chalcopyrite, selenium impurity is absent (see Table 2).

It should be noted that single, very small segregations of acanthite were discovered during the

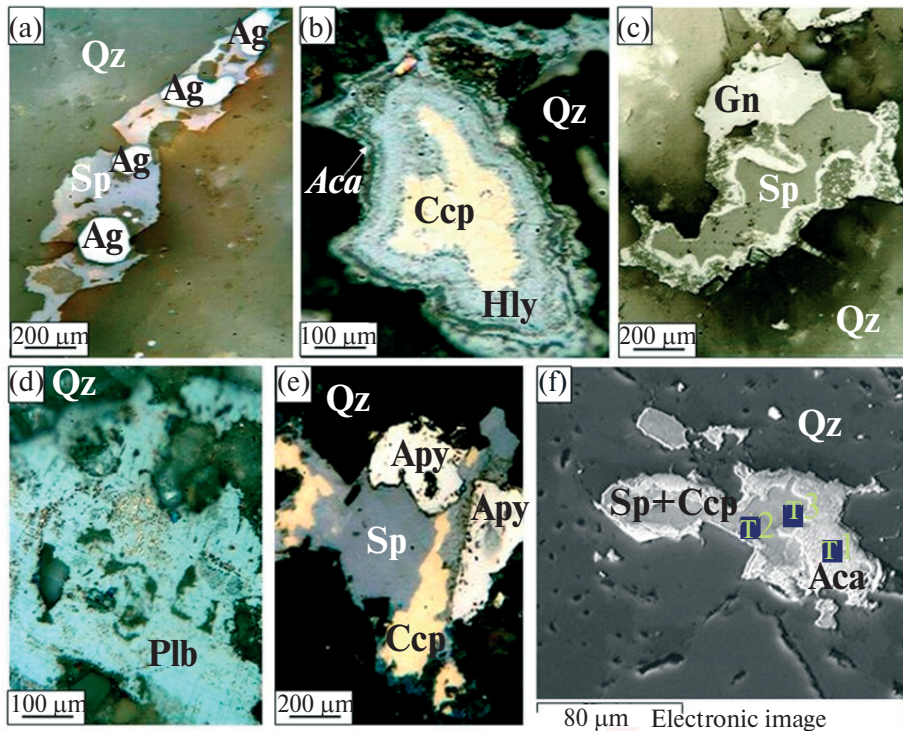


**Fig. 6.** Ore minerals of productive quartz-adularia veins of the Pechalnoe deposit.

a – inclusions of native silver in sphalerite; b – segregation of chalcopyrite with chalcocite rim (on the outer framing, a thin rim of selenium-free hypergene acanthite); c – intergrowth of galena with sphalerite; d – polybasite segregation with characteristic droplets of native silver; e – intergrowth of sphalerite with chalcopyrite and arsenopyrite; f – rim of acanthite (light) on segregation of chalcopyrite with sphalerite (dark) (electron image).

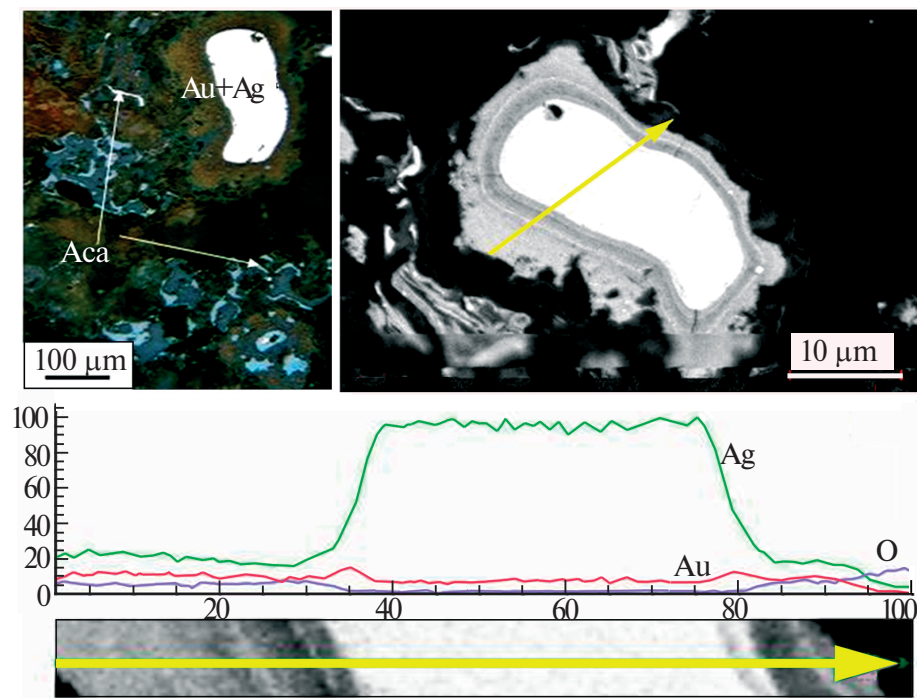


**Fig. 7.** The segregation of native gold in oxidized arsenical pyrite, with a diffusion rim around the native gold. In addition to native gold, highly seleniferous acanthite segregations are identified (left – optical image, right – electron image).

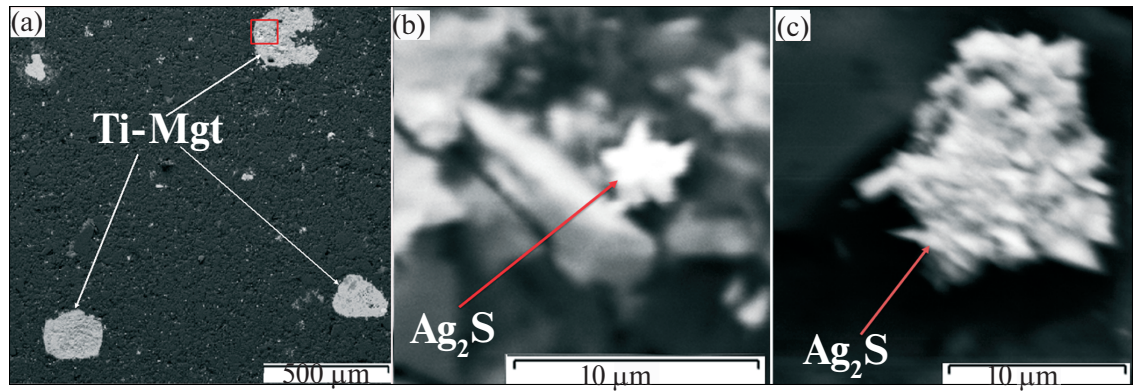


**Fig. 8.** Acanthite segregation in comendites of the Pechalnoe deposit.

a – porphyritic phenocrysts of titanomagnetite (Ti–Mgt) in rhyolites; b, c – acanthite segregation in Ti–Mgt.

study of comendites containing REE mineralization, at a considerable distance from the ore bodies of the deposit (Fig. 8a). Acanthite inclusions are found in titanium-magnetite crystals, which are common in the rock (see Fig. 8a). The inclusions represent clusters of acanthite microcrystals, the size of which is within 1–3  $\mu\text{m}$  (see Fig. 8b, 8c).

Titanomagnetite crystals, almost completely replaced by iron hydroxides and enriched with silicon and aluminum. According to X-ray spectral

analysis, in addition to silver, titanomagnetite crystals are enriched with Nb, Zn and Pb, with Nb being part of the titanomagnetite composition, while Zn and Pb occur in titanomagnetite as sulfates.

#### GEOCHEMICAL FEATURES OF ORES

In the composition of the studied samples of Au–Ag ores from the Pechalnoe deposit,

**Table 3.** Chemical composition of Au–Ag ores of the Pechalnoe deposit (in wt. %)

Components	Sample number					
	PC-1	PC-2	PC-4	PC-5	PC-6	PC-7
SiO <sub>2</sub>	83.68	80.88	80.95	95.96	97.55	76.52
TiO <sub>2</sub>	0.02	0.35	0.49	0.02	0.01	0.64
Al <sub>2</sub> O <sub>3</sub>	8.7	9.9	10.4	1.7	0.21	12.11
Fe <sub>2</sub> O <sub>3</sub>	0.23	3.91	2.48	0.8	1.04	4.93
MnO	0.006	0.018	0.017	0.007	0.05	0.033
MgO	<0.10	0.66	0.58	0.11	<0.10	1.0
CaO	<0.10	<0.10	0.12	<0.10	0.17	0.14
Na <sub>2</sub> O	0.18	0.23	0.15	0.1	<0.10	0.21
K <sub>2</sub> O	7.05	3.04	3.09	0.81	0.14	3.02
P <sub>2</sub> O <sub>5</sub>	0.02	0.12	0.19	0.11	0.06	0.12
S	0.07	0.48	0.61	0.29	0.63	1.17
$\Sigma$	99.956	99.588	99.077	99.907	99.86	99.893

$\text{SiO}_2$  predominates (76.52–95.96%), there are significant concentrations of  $\text{Al}_2\text{O}_3$  (up to 12.11%),  $\text{Fe}_2\text{O}_{3\text{total}}$  (0.23–4.93),  $\text{K}_2$  (0.14–7.05) (Table 3). This indicates that quartz predominates in the composition of ore bodies, with notable amounts of adularia and hydromica present. The ores are characterized by low and very low values of  $\text{Na}_2\text{O}$ ,  $\text{CaO}$ ,  $\text{MgO}$ ,  $\text{TiO}_2$ ,  $\text{P}_2\text{O}_5$  and  $\text{MnO}$  (see Table 3). According to the table, the content of sulfides in the studied ores is small ( $\text{S}_{\text{total}}$  – from 0.7 to 1.17%), which confirms the sulfide-poor nature of the identified mineralization, typical for ores of the epithermal gold-silver formation.

Au–Ag ores of the Pechalnoe deposit (Fig. 9) are characterized by evident enrichment with a fairly wide range of elements (by rating): Ag, Au, As, Sb, Se, W, Tl, Li, Be, Bi, Cs, Mo, compared to the average values of the upper crust Taylor, McLennan, 1988]. Enrichment coefficients vary from several times (W, Tl, Li, Be, Bi) to hundreds (Sb, Se) and thousands (Ag, Au, As) times (see Fig. 9), which is explained by the geochemical affinity of a number of elements and their synchronous participation in ore formation.

The U/Th ratio (Table 4) in the studied ores is almost 2 times less than 0.75 (varying from 0.02 to 0.42), which indicates an oxidizing environment of their ore formation Jones, Manning, 1994].

The Y/Ho ratio of the studied ores varies from 24.12 to 28.58 (see Table 4), which corresponds to the range of ratios characteristic of modern hydrothermal fluids of back-arc basins Monecke et al., 2002].

Light REEs transfer to the aqueous fluid with increasing pressure, while heavy REEs are retained in the magma, allowing the former to be considered “hydrophilic” and the latter “magmaphilic” elements [Zharikov et al. 1999]. Additionally, REEs were divided into three groups: cerium – La, Ce, Pr, Nd, yttrium – Sm, Eu, Gd, Dy, Ho, scandium – Er, Yb, Lu [Mineev, 1974]. According to Table 4, the REE spectra of the studied ores are dominated by light “hydrophilic” lanthanides of the “cerium” group.

Chondrite-normalized REEs of epithermal ores form weakly inclined near-chondritic patterns (Fig. 10), largely similar in configuration to REE patterns of terrigenous rocks of the Verkhoyansk complex [Mikhailitsyna, Sotskaya, 2020] and are characterized by the absence of Eu minima. Consequently, it can be assumed that the REE content in the ores is inherited from the host terrigenous hornfelsed rocks of the lower tier of the VDS.

In the ores of the Pechalnoe deposit,  $\Sigma\text{REE}$  varies widely (from 1.17 to 84.78 g/t) (see Table 4). Such intervals of REE concentration totals are characteristic of epithermal ores from other OChVB deposits with breccia textures [Volkov et al., 2018].

In samples from the Pechalnoe deposit ores, the values of  $\text{Eu/Eu}^*$  and  $\text{Ce/Ce}^*$  vary from negative to slightly positive (see Table 4). This combination of  $\text{Eu/Eu}^*$  and  $\text{Ce/Ce}^*$  also indicates oxidizing conditions that existed during ore deposition [Goryachev et al., 2008].

Low Eu/Sm ratios (<1) in the studied ores (see Table 4) show that ore formation occurred at the upper crustal level [Vinokurov, 1996].

## DISCUSSION OF RESULTS AND CONCLUSION

The Pechalnoe deposit generates significant interest as it formed in carbonaceous terrigenous strata of the VDS basement, at a distance of about 200 km from the OChVB. Terrigenous sequences at the base of volcanic structures are traditionally considered an unfavorable environment for the localization of epithermal volcanic mineralization [Helke, 1946; Schneiderhöhn, 1958]. In particular, G. Schneiderhöhn [1958] believed that epithermal gold and Au–Ag deposits form a separate group and have their own special roots in subvolcanic intrusions; transitions to mesothermal plutonogenic deposits were denied, and the absence of epithermal ores without connection to igneous rocks was indicated.

In a summary of the South Carpathian gold-bearing province, A. Helke [1946] wrote that in the black Mediterranean shales underlying the volcanics, Au–Ag veins wedge out, penetrating them to a depth

of 50 m. However, Au–Ag epithermal deposits such as Vysokovoltnoye and Kosmanychi (Central Kyzylkum), Baley and Taseevka (Transbaikalia), Promezhutochnoye (Central Chukotka) are located in terrigenous strata.

The richest deposit, Hishikari (more than 250 tons of gold, with an average content of 60 g/t) in Japan, is also located in terrigenous strata at the base beneath a cover of volcanic rocks [Izava et al., 1990]. Productive quartz-adularia veins of the Pechalnoye deposit are also located in terrigenous strata under a volcanic screen. However, with the exception of the Balei and Hishikari deposits, all others are classified as small in terms of reserves.

Currently, the connection of Au–Ag epithermal deposits with island-arc and post-accretionary volcanic belts, with flattening subduction, rift structures, and post-collisional back-arc extension is recognized [Richards, 2013]. The formation of the Pechalnoye deposit is associated with the latter setting.

In the generally accepted classification [White, Hedenquist, 1995], epithermal deposits are divided into two types based on the oxidation state of sulfur in hydrothermal fluids: low-sulfidation (LS) and high-sulfidation (HS). Later, another type was identified [Hedenquist et al., 2000] — intermediate-sulfidation (IS). LS-type deposits are typically characterized [Hedenquist et al., 2000] by a pyrite-pyrrhotite-arsenopyrite mineral complex with iron-rich sphalerite. As a result of research, the following mineralogical characteristics of the ores of the Pechalnoe deposit have been established: low sulfide content of ores (1–2%); the main ore-forming minerals are native silver, low-grade gold, polybasite, and highly seleniferous acanthite, in addition, arsenical pyrite, arsenopyrite, pyrrhotite, iron sphalerite, chalcopyrite and marcasite are quite widely developed in the ores.

The results of geochemical studies of ores correspond with mineralogical data. Notable enrichment of epithermal ores with a fairly wide range of trace elements (by rating): Ag, Au, As, Sb, Se, W, Tl, Li, Be, Bi, Cs, Mo, predominance of light lanthanides over heavy ones, very low Eu/Sm ratios (<<1), slightly

inclined near-chondritic spectra without europium minima or maxima — are typical for the epithermal ore-forming system of the Pechalnoe deposit. And the ratio of Ce/Ce\* and Eu/Eu\* values indicate oxidizing conditions that prevailed during ore formation. The distribution of REE in epithermal ores is largely similar in configuration to the REE spectra of the host terrigenous rocks of the Verkhoyansk complex [Mikhailitsyna, Sotskaya, 2020].

The REE spectra are dominated by light “hydrophilic” lanthanides of the “cerium” group. ΣREE varies widely. High values of ΣREE are characteristic of breccias, and low values — for quartz-adularia veins. Therefore, it can be assumed that the content of REE in ores depends on the amount of fragments of host terrigenous hornfelsed rocks of the lower tier of the VDS. Increased arsenic and selenium content of Au–Ag ores of the deposit, very likely, inherited from enriched As and Se carbonaceous terrigenous host rocks of the base of VDS [Savva, 2005; Volkov et al., 2006]. The obtained mineralogical and geochemical data allow attributing the mineralization of the Pechalnoe deposit to the selenium subtype of the low-sulfidation type of epithermal deposits.

As a result of the conducted research, the following model for the formation of the Pechalnoe deposit can be proposed. During the pre-productive stage, due to the emplacement of the Upper Orotukan intrusive of leucocratic granites and comagmatic dikes and stocks of Late Cretaceous age, veins of gray medium-grained quartz were formed, which are located in greisens and greisenized rocks and are accompanied by tin mineralization. Epithermal Ag–Au veins of the productive stage are associated with the formation of volcanic rocks of the basalt-rhyolite formation of Late Cretaceous age. This stage includes quartz and quartz-adularia Ag–Au veins, closely associated with metasomatites of the secondary quartzite formation.

As a result of mineralogical and geochemical studies, it can be assumed that the formation of Ag–Au mineralization occurred after the intrusion of rhyolites of the first phase, which screen the productive veins, and before the

**Table 4.** Elemental composition (g/t) of Au–Ag ores from the Pechalnoe deposit

Sample No.	PC-1	PC-2	PC-4	PC-5	PC-6	PC-7
Au	13.20	0.24	0.16	1.72	1.06	1.13
Ag	487.40	19.51	9.85	116.93	3.66	2.84
As	53.67	2356.05	7476.51	206.18	486.00	558.56
Sb	20.88	29.19	292.68	83.15	35.15	26.44
Cu	3.32	16.53	19.65	15.85	7.90	28.66
Pb	31.72	5.77	15.00	10.51	1.90	16.30
Zn	15.71	50.72	66.95	89.21	79.00	56.00
Li	155.11	204.84	149.01	148.08	98.19	157.06
Be	109.44	2.80	2.34	8.36	3.59	4.11
Sc	<0.1	2.05	1.13	<0.1	<0.1	6.94
V	<0.1	20.76	34.49	<0.1	<0.1	65.11
Cr	5.37	41.37	39.81	91.34	67.63	56.79
Co	0.26	<DL	1.28	0.09	0.13	0.35
Bi	1.70	0.23	0.44	1.23	0.25	0.93
Ga	15.21	26.94	17.93	15.59	9.75	26.40
Rb	592.30	260.32	161.99	73.78	9.17	205.59
Sr	7.14	57.05	13.24	28.45	12.64	37.06
Y	0.31	11.86	8.23	0.73	0.06	15.52
Zr	1.99	57.93	82.84	2.67	0.36	120.51
Nb	<0.003	4.33	7.44	<0.003	<0.003	8.27
Mo	3.17	22.41	<0.018	0.16	0.90	<0.018
Sn	0.35	<DL	<DL	3.54	<DL	<DL
Cs	18.09	35.57	21.75	15.18	3.77	32.70
Ba	41.15	286.73	148.84	45.21	47.09	315.85
La	0.23	16.21	11.28	2.64	2.69	16.35
Ce	0.28	35.14	22.22	4.33	2.66	33.65
Pr	0.07	4.30	3.00	0.41	0.16	4.03
Nd	0.36	16.22	10.78	1.15	0.39	14.84
Sm	0.05	3.22	2.22	0.18	0.03	3.19
Eu	0.02	0.71	0.40	0.04	<DL	0.70

**Table 4.** *Continued*

Sample No.	PC-1	PC-2	PC-4	PC-5	PC-6	PC-7
Gd	0.04	2.79	1.70	0.07	<DL	2.42
Tb	0.01	0.44	0.27	0.02	0.00	0.44
Dy	0.06	2.42	1.52	0.10	0.00	2.53
Ho	0.01	0.49	0.33	0.03	<0.0002	0.56
Er	0.03	1.32	0.92	0.07	0.01	1.87
Tm	0.00	0.17	0.13	0.01	<DL	0.31
Yb	0.01	1.22	0.89	0.05	0.01	1.96
Lu	<DL	0.16	0.13	0.01	<DL	0.29
Hf	<0.003	1.58	2.51	<0.003	<0.003	3.37
Ta	<0.001	0.22	0.42	<0.001	<0.001	0.46
W	7.34	28.92	17.85	15.49	0.63	36.94
Tl	19.44	4.72	4.73	2.19	3.74	6.34
Th	<0.002	4.05	2.98	0.14	0.17	5.63
U	0.04	1.14	1.22	0.04	0.00	1.78
$\Sigma$ REE	1.17	84.78	55.80	9.09	5.95	83.15
$\Sigma$ LREE	1.01	75.79	49.91	8.75	5.93	72.77
$\Sigma$ HREE	0.17	8.99	5.89	0.34	0.02	10.38
$\Sigma$ LREE/ $\Sigma$ HREE	6.05	8.43	8.47	25.54	254.62	7.01
Y/Ho	28.58	24.13	24.99	26.83	27.48	27.48
U/Th	0.28	0.28	0.41	0.25	0.02	0.32
Rb/Sr	82.91	4.56	12.24	2.59	0.72	5.55
Au/Ag	0.03	0.01	0.02	0.01	0.29	0.40
Eu/Eu*	1.09	0.80	0.71	0.85	0.80	0.80
Ce/Ce*	0.61	1.08	0.99	0.90	0.57	1.03
$\Sigma$ Ce	0.94	71.86	47.28	8.53	5.90	68.88
$\Sigma$ Y	0.19	10.06	6.45	0.43	0.04	9.85
$\Sigma$ Sc	0.05	2.86	2.07	0.13	0.02	4.43
Eu/Sm	0.34	0.22	0.18	0.21	0.22	0.22

Note. Determination of elements and REE by inductively coupled plasma mass spectrometry (ICP-MS) , Shared Research Facility Analytical Center of IGEM RAS; DL – detection limit; REE – rare earth elements; LREE – light rare earth elements; HREE – heavy rare earth elements.

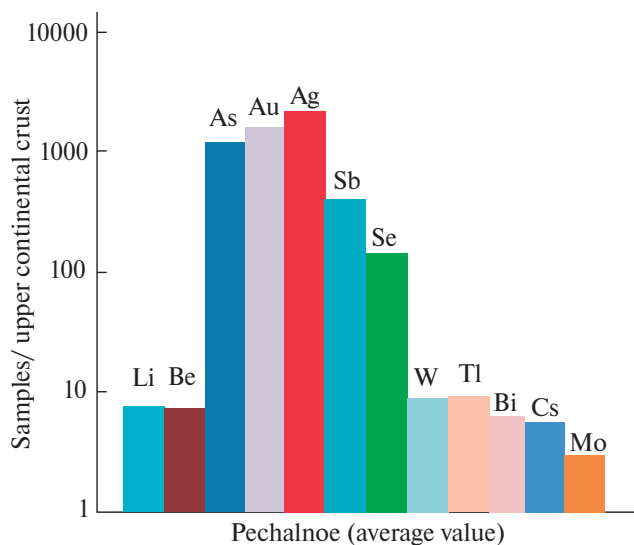


**Fig. 9.** Distribution of major trace elements in the studied samples of Au–Ag ores from the Pechalnoye deposit, normalized to the average values for the upper crust [Taylor, McLennan, 1988]. Average of 6 samples (see Table 4).

intrusion of fluid rhyolites and comendites of the second phase, containing rare metal and REE mineralization. This sequence is confirmed by low REE contents in productive veins, as well as the absence of similarity between REE spectra in productive veins and in REE-containing rhyolites and comendites [Volkov et al., 2023].

The productive veins of the Pechalnoe deposit are practically not eroded, as most of them are localized under the screen of the Pechalninsky

volcanic sequence. The depth of ore mineralization, by analogy with other objects (Hishikari), may exceed 200 m. Among the mineralogical signs of minor erosional truncation, it is worth noting the widespread development of colloform-banded textures and adularia in veins, as well as the insignificant amount of polymetallic mineralization in ores [Savva, 2018]. Weak erosion suggests a high probability of identifying ore bodies that do not reach the surface.

The obtained results can be used in regional and local forecasting-metallogenetic constructions, prospecting, and evaluation of new epithermal Au–Ag deposits. Given the poor exploration of the feathering zones of the TMA of the Okhotsk sector of the OCVB, they have high prospects for the discovery of new epithermal Au–Ag and Ag deposits.

## ACKNOWLEDGEMENTS

The authors express their deep gratitude to the geologist of JSC “Polymetal MC” Sergey Fedorovich Petrov for providing a collection of ore samples from the Pechalnoe deposit for research.

## FUNDING

The work was carried out with the financial support of the State Assignment of IGEM RAS (State registration № 124022400144-6).

## CONFLICT OF INTEREST

The authors of this work declare that they have no conflict of interest.

## REFERENCES

1. Vinokurov S.F. Europium anomalies in ore deposits and their genetic significance // DAN. 1996. Vol. 346. No. 6. pp. 792–795.
2. Volkov A.V., Goncharov V.I., Sidorov A.A. Deposits of gold and silver Magadan: NEISRI FEB RAS, 2006. 221 p.
3. Volkov A.V., Sidorov A.A., Prokofiev V.Yu., Savva N.E., Kolova E.E., Murashov K.Yu. Features of epithermal

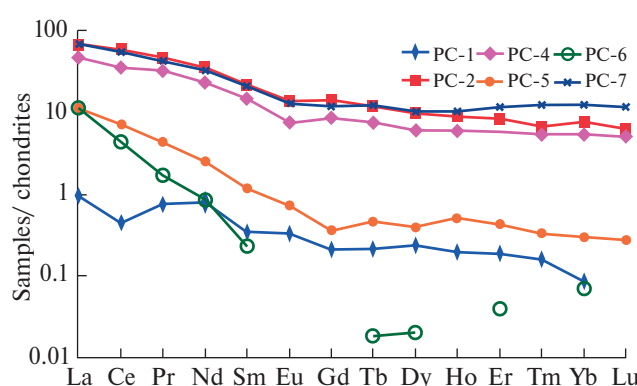


**Fig. 10.** Distribution of REEs normalized to chondrites [McDonough, Sun, 1995], in Au–Ag ores of the Pechalnoe deposit. Sample numbers correspond to Tables 3, 4.

ore formation of the Okhotsk-Chukotka volcanic-plutonic belt (North-East Russia) // *Volcanology and Seismology*. 2018. No. 6. Pp. 3–22.  
DOI: 10.1134/S0203030618060093

4. *Volkov A.V., Galyamov A.L., Murashov K.Yu.* Alkaline rhyolites of the Pechalninsky ore field (North-East Russia) – a potential large-volume source of heavy rare earth elements // *Doklady RAS. Earth Sciences*. 2023. Vol. 510. No. 1. Pp. 46–51. DOI: 10.31857/S2686739723600054

5. *Goryachev N.A., Vikentieva O.V., Bortnikov N.S., Prokofiev V.Yu., Alpatov V.A., Golub V.V.* The world-class Natalkinskoye gold deposit: REE distribution, fluid inclusions, stable oxygen isotopes and ore formation conditions (North-East Russia) // *Geology of Ore Deposits*. 2008. Vol. 50. No. 5. Pp. 414–444.

6. *Egorov V.N., Zhigalov S.V., Volkov A.V., Sidorov A.A.* On rare metal mineralization in trachyrhyolites and comendites of the Khurchan-Orotukan metallogenic zone // *DAN*. 2005. Vol. 405. No. 2. Pp. 237–242.

7. *Zharikov V.A., Gorbachev N.S., Latfut P., Doherty V.* Distribution of rare earth elements and yttrium between fluid and basaltic melt at pressures of 1–12 kbar (according to experimental data) // *Dokl. RAS*. 1999. Vol. 366. No. 2. Pp. 239–241.

8. *Kuznetsov V.M., Nishchansky G.M., Palymskaya Z.A.* Signs of manifestation and forms of expression of tectonomagmatic activation on the example of the Khurchan-Orotukan zone // *Kolyma*. 1993. No. 7. Pp. 7–12.

9. *Kuznetsov V.M., Zhigalov S.V., Vedernikova T.A., Shpikerman V.I.* State geological map of the Russian Federation. Scale 1:1,000,000 (third generation). Verkhoyano-Kolyma Series. Sheet P-56 – Seimchan. Explanatory note. St. Petersburg: Cartographic Factory VSEGEI, 2008. 426 p.

10. *Mineev D.A.* Lanthanides in ores of rare earth and complex deposits. Moscow: Nauka, 1974. 241 p.

11. *Mikhailitsyna T.I., Sotskaya O.T.* The role of black shale strata in the formation of the Natalka and Pavlik gold deposits (Yano-Kolyma orogenic belt) // *Geology and Geophysics*. 2020. Vol. 60. No. 12. Pp. 1648–1671.  
DOI: 10.15372/GiG2020149

12. *Savva N.E.* On the possible source of selenium in volcanic deposits // *Science of the North-East Russia – beginning of the century* // Materials of the All-Russian scientific conference dedicated to the memory of academician K.V. Simakov and in honor of his 70th anniversary (Magadan, 26–28 April 2005). Magadan: NESC FEB RAS, 2005. Pp. 208–210.

13. *Savva N.E.* Mineralogy of silver in the North-East of Russia. Moscow: Triumph, 2018. 544 p.

14. *Sidorov A.A.* Gold-silver formation of the East Asian volcanogenic belts. Magadan, 1978. 368 p.

15. *Taylor S.R., McLennan S.M.* Continental crust: its composition and evolution. Moscow: Mir, 1988. 384 p.

16. *Khelke A.* Young volcanogenic gold-silver deposits of the Carpathian arc. Moscow: Publishing House of the All-Union Chamber of Commerce, 1946. 350 p.

17. *Schneiderhen G.* Ore deposits. Moscow: Foreign Literature, 1958. 450 p.

18. *Grigorieva A.V., Volkov A.V., Sidorova N.V.* REE Mineralization in Alkaline Rhyolites of the Pechalninskii Ore Field (Northeast Russia) // *Doklady Earth Sciences*. 2024. <https://doi.org/10.1134/S1028334X24601469/>

19. *Hedenquist J.W., Arribas A., Gonzalez-Urien E.* Exploration for epithermal gold deposits. Gold in 2000 // *Reviews in Economic Geology*. Littletown, Society of Economic Geologists. 2000. Pp. 245–277.

20. *Izava E., Urashima Y., Ibaraki K.* The Hishikari gold deposits: high-grade epithermal veins in Quaternary volcanic of southern Kyushu, Japan // *Journal of Geochemical Exploration*. 1990. Vol. 36. Pp. 1–56.

21. *Jones B., Manning D.A.C.* Comparison of geochemical indices used for the interpretation of palaeoreodox conditions in ancient mudstones // *Chem. Geol.* 1994. Vol. 111. Pp. 111–129.

22. *McDonough W.F., Sun S.S.* The Composition of the Earth // *Chem. Geol.* 1995. Vol. 120. Pp. 223–253.

23. *Monecke T., Kempe U., Gotze J.* Genetic significance of the trace element content in metamorphic and hydrothermal quartz: a reconnaissance study // *Earth Planet. Sci. Lett.* 2002. Vol. 202. Pp. 709–724.

**24.** *Richards J.P.* Giant ore deposits formed by optimal alignments and combinations of geological processes // *Nat. Geosci.* 2013. Vol. 6. Pp. 911–916.

**25.** *White N., Hedenquist J.* Epithermal gold deposits: Styles, characteristics and exploration // *SEG News Letter.* 1995. No. 23. Pp. 1–12.